

Glossiness distribution over the surface of stoneware floor tiles due to the polishing process

Fábio Jose Pinheiro Sousa · Nério Vicente Júnior ·
Walter L. Weingaertner · Orestes E. Alarcon

Received: 25 August 2006 / Accepted: 15 August 2007 / Published online: 23 September 2007
© Springer Science+Business Media, LLC 2007

Abstract The industrial process for polishing floor tiles requires several polishing stages in order to produce the desirable glossiness. Works on floor tile polishing with focus on the distribution of glossiness still lack in literature. The present work intends to measure and analyze the distribution of glossiness over the surface of porcelain stoneware tiles polished using forward speed of 7.5 cm s^{-1} and lateral oscillation frequency and amplitude of 0.2 s^{-1} and 12 cm. The glossiness pattern generated by the polishing process over the surface of six tiles were presented in grey-scale graphics, where each pixel was univocally associated with a portion of the tile surface. Correlations between the glossiness pattern found and the polishing kinematics were developed. Significant differences of glossiness were registered either between tiles polished under the same polishing condition, or within the surface of the same tile, between adjacent regions. The use of lateral oscillation motion caused the glossiness pattern over the tile surface to follow a waveform pattern, and two corroborative hypotheses were made in order to explain such fact, considering the light-surface interaction as well

as the overlapping of trajectories of adjacent polishing heads.

Introduction

The industrial process for polishing porcelain stoneware tiles involves several steps, equipments and parameters. Often more than 30 polishing machines are disposed in sequence to result in an industrial polishing train, in order to lead the tile surface to the desirable glossiness, which is the most important criterion to control the quality of such products [1].

Recently many fruitful works on this subject are available in literature [2–6]. However, these works either deal with mean values taken from random positions on the tile surface, or do consider only the distribution of glossiness for tiles polished without using the lateral oscillation motion of the polishing heads. The distribution of glossiness for porcelain stoneware tiles polished using lateral oscillation motion still lacks in literature.

As lateral oscillation uses to be available in mostly modern polishing machines, the present work intends to measure the corresponding distribution of glossiness. Moreover, an attempt to make some correlations between the glossiness pattern found and the kinematics involved in tile polishing process were carried out. The available motion considered in polishing trains can be seen in Fig. 1.

Each polishing head is mounted by a horizontal spinning plate in which six abrasive blocks are coupled keeping a radial symmetry. These abrasive blocks are magnesium oxychloride bounded containing innumerable silicon carbide particles, which work as abrasive particles [4, 5, 7].

F. J. P. Sousa (✉)
Post graduation Program in Material Science & Engineering –
PGMat, Department of Mechanical Engineering – EMC, Federal
University of Santa Catarina – UFSC, CP 476, Campus
Universitário Trindade, Florianópolis, SC CEP 88040-900,
Brazil
e-mail: fabiodacivil@pg.materiais.ufsc.br

N. V. Júnior
Undergraduate in Materials Science and Engineering – EMC,
UFSC, Florianópolis, SC, Brazil

W. L. Weingaertner · O. E. Alarcon
Department of Mechanical Engineering – EMC, UFSC,
Florianópolis, SC, Brazil

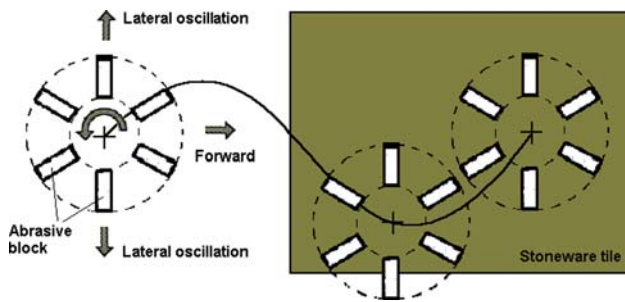


Fig. 1 Plan view of the polishing head indicating the relative motion

The trajectory of the active abrasive particles is governed by the preset motion of the polishing head, just as presented in Fig. 1. As consequence favoured regions of material removal usually occur. For simple polishing machines, in which no lateral oscillation is available, the centre of tile undergoes a gentler polishing than the tile boundary, due to the lacking of abrasive in the middle of polishing heads. This difference leads to the profile of abrasive contact showed in Fig. 2, already well known [4, 5].

As the glossiness is somehow caused by the abrasive contacts, it is reasonable to expect a glossiness pattern as the one exemplified in Fig. 2. Such patterns are colloquially known as “polishing shadows” and are usually sharp enough to be detected by operators that can often say the direction in which tiles were polished.

To improve the gloss distribution exhibit in Fig. 2 a lateral oscillation movement was introduced in the nearest generation of polishing trains. For such modern trains, the distribution of abrasive contacts also varies as function of the lateral oscillation motion. Considering the trajectory of a single abrasive particle a zigzag overlapping is found to occur, as presented in Fig. 3. Further details on the kinematics of a single abrasive during the polishing process of porcelain stoneware tiles can be found elsewhere [8].

Figure 3 actually presents a continuous scratch acting during polishing. The graphic was analytically determined using parameters found in literature [4, 5] and typically adopted. Nevertheless, later it will also be used data collected from an industry of ceramic tiles in Brazil, country with world-level participation in the market of ceramic tiles [9].

Fig. 2 Profile of the number of abrasive contacts promoted by a simple polishing head

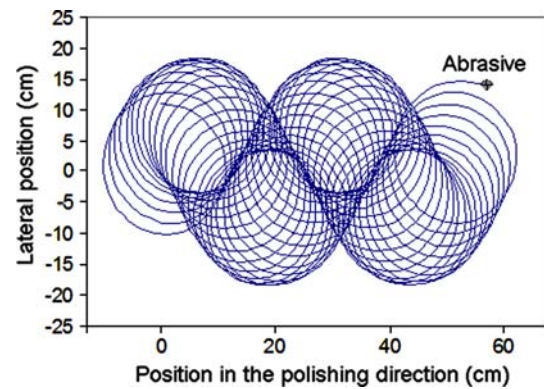
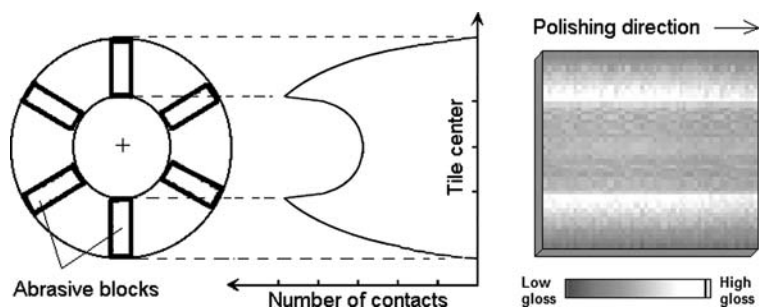


Fig. 3 Trajectory of a single abrasive during polishing

The polishing head was represented hereafter by its central point (point C). The axis presented in Fig. 4 was adopted so that the resulting trajectory of the polishing head regarding an arbitrary origin (point O) could be achieved.

Vector \vec{OC} results in fact from the sum of the forward motion vector and the lateral oscillation vector, each one in the direction of \hat{i} and \hat{j} respectively. Mathematically:

$$\vec{OC} = \{V \cdot t\} \cdot \hat{i} + \left\{ \frac{A}{2} \cdot \sin(2 \cdot \pi \cdot f \cdot t) \right\} \cdot \hat{j} \quad (1)$$

where V is the forward speed of the polishing train [ms^{-1}], f is the frequency of the lateral oscillation [s^{-1}], A is the lateral oscillation amplitude [m] and t is time [s]. Although the rotation of the abrasive disc [rad/s] leads also to movement of the abrasive blocks, it causes no motion of point C, and therefore it was not included in Eq. 1.

Equation 1 represents a wave function to be followed by each polishing head in the polishing train, so that the whole polishing train accomplishes the same movement together. Since the time spent in each complete cycle of lateral oscillation motion is by definition $T = 1/f$, the length λ of the generated wave can be taken directly as:

$$\lambda = \frac{V}{f} \quad (2)$$

Nevertheless, because of the distance L between adjacent polishing heads, there is a phase delay between

Fig. 4 Trajectory of the centre point of a polishing head due to the available motions

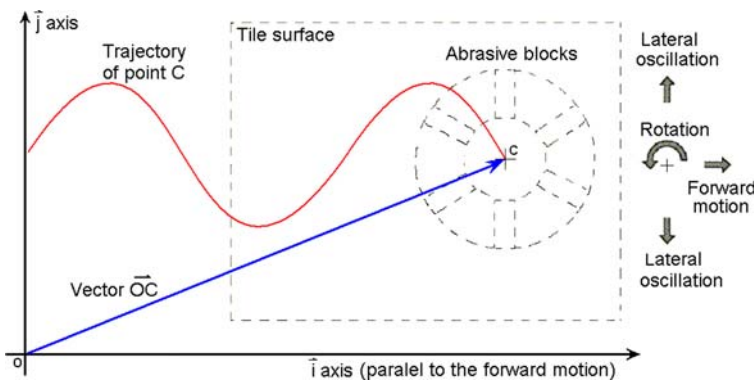
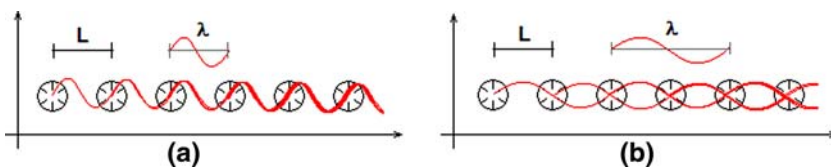


Fig. 5 Overlapping of polishing heads: (a) constructive and (b) destructive interferences



waves from successive polishing heads. Therefore an analogy to coherent waves can be employed. Either full or partial interference may occur depending on L and λ , as seen in Fig. 5.

In case of full constructive interference, Fig. 5a, all the polishing heads work on the same place. This is considered undesirable since it would also lead to a sharp glossiness pattern over the tile surface. In other words some areas would be overworked whereas others would be poorly polished. Depending on the dimensions of tiles and polishing heads, regions with no contact would result.

Experimental

The sequence of abrasive size adopted in the polishing train is presented in Fig. 6. It was used 36 polishing heads and 18 different abrasive sizes to accomplish the polishing process. This final sequence was reached by the expertise of employees, just like typically occurs in most floor tiles polishing industries [3].

A commercial type of stoneware floor tile named Galileu Crema, made by *Cerâmica Portobello* Company, was analyzed. The following kinematic conditions were adopted: forward speed $V = 7.5 \text{ cm s}^{-1}$, lateral oscillation

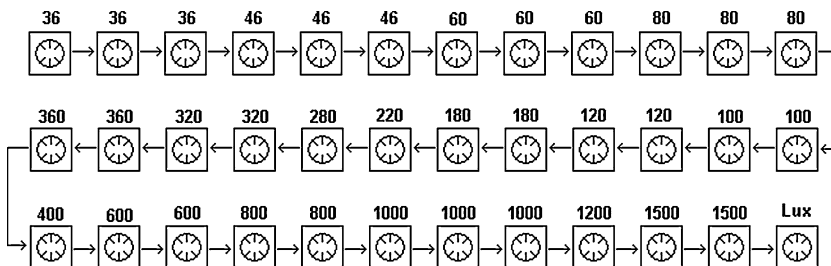
frequency $f = 0.2 \text{ s}^{-1}$ and amplitude $A = 12 \text{ cm}$. Outer and inner diameters of the polishing head were 23 and 11 cm respectively.

After the process had approached a stationary behaviour, six complete polished tiles, with nominal dimension of $45 \times 45 \text{ cm}$, were taken in the sequence of production in order to have their glossiness measured.

A glossmeter model IG-320, Mark Horiba, was used for measuring the glossiness all over the tile surface. Grey-scale graphics were used to present the results. In these graphics each portion of the tile surface has a corresponding pixel, whose colour stands for its glossiness. It was adopted a pixel mapping exemplified by Fig. 7. As the glossmeter had a nominal covering area of $25 \times 35 \text{ mm}^2$ for each measuring, this was the size taken to be represented by a single pixel. Nevertheless, the effective measuring area has in fact an oval shape with dimensions of $12 \times 6 \text{ mm}^2$, centred in the nominal covering area [10]. The boundary of each region on the tile surface was carefully marked by a pencil.

The glossiness pattern obtained for those six tiles were then analyzed in order to confirm either a zigzag produced by individual abrasives, as presented in Fig. 3, or a wave pattern promoted by the overlapping of adjacent polishing heads, as exhibited in Fig. 5.

Fig. 6 Sequence of abrasive size adopted



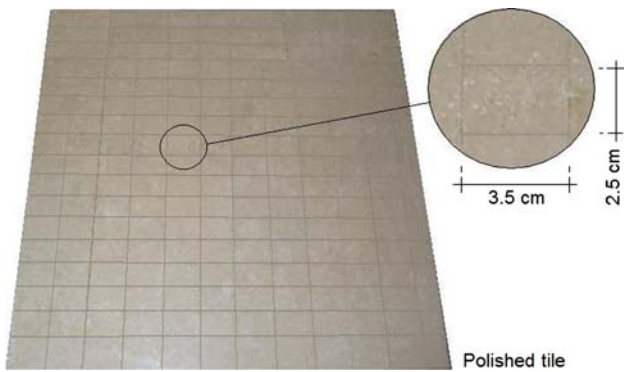


Fig. 7 Pixel mapping

Results and discussion

The glossiness values measured at the six polished tiles are presented in Fig. 8. The lower is the glossiness the darker is the colour presented in graphics, according to the legend. Although all tiles were polished in sequence with no gap between them, the boundaries between adjacent tiles are quite sharp, probably due to the absence of mechanic continuity between them.

As mentioned previously the rectangular shape of each pixel in graphics was defined by the glossmeter. Therefore, in view of the tile dimensions, 12 and 18 pixels are required to represent the width and the length of each tile, respectively.

In spite of all tiles have been submitted to the same polishing condition, some difference on glossiness can be observed between them, even between adjacent tiles. Some possible reasons for this could be the individual characteristics of fired tiles. Surface porosity and microstructure are properties which may vary within tiles, and they are

considered important features to define the final glossiness of the tile [3, 6, 11].

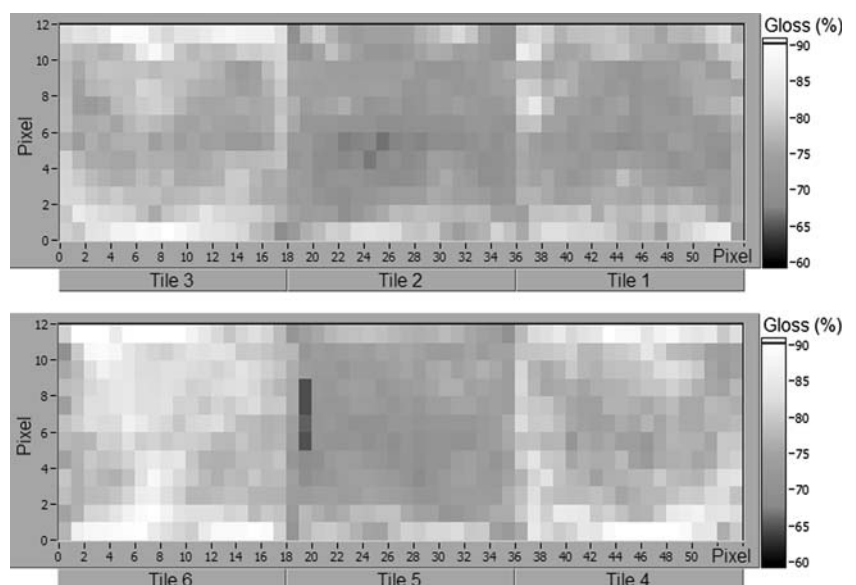
Another possible feature that could result in glossiness differences would be the tile thickness after firing. The polishing process is preceded by a leveling step in order to assure the size regularity of tiles. Nevertheless, it usually causes damages in the tile surface [1, 3, 11], either by exposing closed porous or by generating cracks [12].

Tiles with different thickness are exposed to different penetrations of the grinding tools, so that tiles with different level of surface damage can occur. This in turn could result in different behaviour during the foregoing polishing step. In order to estimate the spatial variation of material removal over the surface of tiles during the levelling, an extra tile was selected and its topography was measured before and after the process, by a coordinate measuring machine, Mark Mitutoyo, model BLNA916. Results are presented in Fig. 9.

Removal depth was found to vary within a very small range between adjacent regions, mostly less than 5 μm. In previous study on superficial damages due to the levelling process, Wang et al. [1] have estimated an average thickness of the damaged layer in about 60 μm. In view of this, the difference of thickness presented in Fig. 9 plays likely a minor role in the difference of glossiness observed.

Figure 8 still reveals another important feature on the gloss distribution. When using the lateral oscillation motion the sharp gloss pattern of Fig. 2 gave places to a less sharp wave pattern of gloss, as can be seen in Fig. 10, which joins all the six measured tiles just in the sequence they were produced. A reference wave was included into the Figure. The properties of this wave were established considering the kinematic parameters adopted for the polishing process, i.e. length λ = 37.5 cm, defined by Eq. 2,

Fig. 8 Glossiness over the surface of six tiles polished using lateral oscillation motion



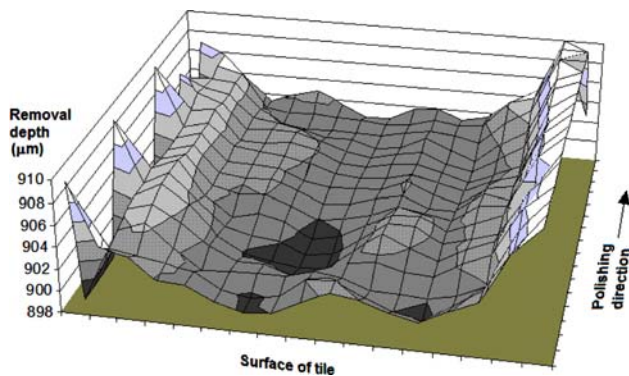


Fig. 9 Removal depth over the tile surface due to leveling step

and amplitude $A = 12$ cm. Therefore, the wave describes the trajectory accomplished by the centre of a given polishing head.

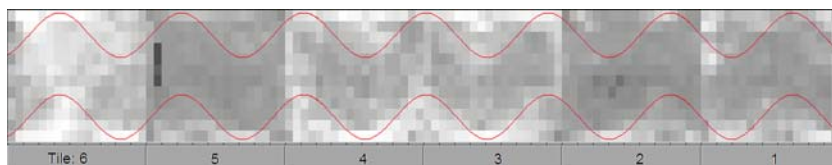
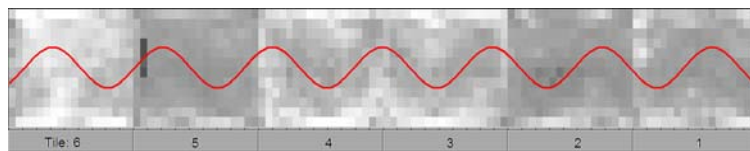
As can be seen, in spite of the differences between individual tiles, the glossiness pattern of the whole set seems to follow the reference wave convincingly. This fact reveals certain relationship between the polishing kinematics and the resulting distribution of glossiness.

Although for single abrasives the central region should undergo more abrasive contacts in function of the kinematic conditions, as indicated in Fig. 4, the lacking of abrasives in the middle of each polishing head explains the lower glossiness found in the central region of the polished tiles. This can be confirmed with aid of Fig. 11. The region corresponding to the passage of the region without abrasive was delimited.

The contrast of glossiness found in the vicinity of the delimitation curves is in fact in agreement with the contact profile exposed in Fig. 2, as the number of abrasive contacts increases abruptly in this region. For the same reason, regions outside the delimitation curves had also presented higher glossiness, for all the six tiles measured. Differences of glossiness up to 10% were found between adjacent pixels located in those curves, and up to 6% between central pixels.

Fig. 10 Wave glossiness pattern exhibited by tiles polished using lateral oscillation motion

Fig. 11 Region with lower glossiness due to lacking of abrasive



On the other hand, the good fitting observed in both Figs. 10 and 11 leads us to the following question: why does the glossiness pattern seems to follow the trajectory of a single polishing head if the polishing process is accomplished by several others polishing heads? An attempt to answer this question was made considering two corroborative hypotheses.

The first hypothesis is related to the gloss gaining along the polishing train, which can be seen in Fig. 12, based on data from literature [11].

First it can be seen that glossiness improvement are mainly promoted in the last stages of the polishing train. Additionally, Fig. 12 highlights that the glossiness of a given tile can increase greatly after certain polishing heads. According to the polishing sequence exhibited in Fig. 6, both the grit size 400 and 1,200 were adopted at only one polishing head, respectively. Thus, taking into account the difficulty found by a given abrasive size in removing the tracks left by coarser abrasives [1, 2, 11], a substantial gloss gaining ascribed by a single polishing head could explain, in some extent, the glossiness pattern obtained.

Such level of individual gloss gaining becomes possible due to the sensitive behaviour of a light beam while it hits onto nearly smooth surfaces. From the point of view of geometric optics, light scattering (diffuse reflection) is

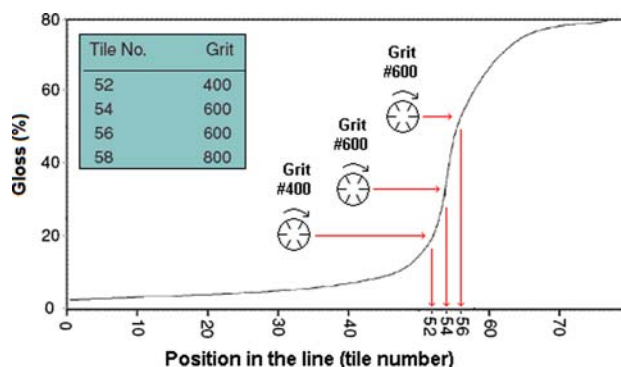


Fig. 12 Abruptly gloss gaining after action of certain polishing heads

expect for rough surfaces, whereas reflection of light in a single beam of specific direction (specular reflection) may prevail for smooth surfaces.

The Rayleigh criterion is usually taken into account to classify between polished and rough surfaces. Briefly, this criterion considers that the presence of asperities generates different optical paths for adjacent coherent waves, which leads to phase differences between them. A surface should be considered polished if the height of its asperities, commonly represented by the surface roughness R_a , leads to a phase difference of less than $\pi/2$ [14]. This reasoning was expressed in Eq. 3:

$$R_a \leq \frac{\lambda}{8 \cdot \cos \theta} \tag{3}$$

where λ is the wavelength of the incident light and θ is the incident angle. Both parameters depend on the glossmeter adopted, furnished by the manufacturer as $\lambda = 0.880 \mu\text{m}$ and $\theta = 60^\circ$ [10].

After replacing λ and θ , Eq. 3 leads to $R_a = 0.22 \mu\text{m}$. This value is pretty close to the surface roughness that can be found in literature [1, 5, 6] for surface of tiles after grit 400. Such fact therefore explains why a markedly increase of gloss can occur even after a little reduction on the surface roughness promoted by a single polishing head.

In addition, a similar gloss gaining behaviour was found by Huang et al. [15] while studying the polishing of two different types of granite. In their studies the same value of $0.2 \mu\text{m}$ was empirically adopted as limit of surface roughness under which the glossiness undergoes an exponential increase.

Further glossiness improvement goes on until it approaches an asymptotically limit established by the tile microstructure [3, 6, 11]. However, due to the minimal reduction on surface roughness in the final polishing steps, the relationship between surface roughness and glossiness in such stages becomes not obvious [1]. This fact was still verified in this work by using the experimental approach exposed in Fig. 13.

Considering only the surface of Tile 1 10 pixels with glossiness from 68 to 88% were selected. Eight profiles of roughness of 5.6-mm length were carried out at the centre

of each selected pixel, considering the orientations exposed in Fig. 13.

The roughness R_a was calculated for each orientation and the arithmetical average of these values was then used to represent each pixel. A perthometer model M2 mark Mahr was used. An example of roughness profile typically obtained can be seen in Fig. 14.

As shown in Fig. 14 the polished surface presents a very smooth surface. In general only a few values are more than $1\text{-}\mu\text{m}$ deep, related to the presence of pores. Such pores were excluded in the estimative of roughness, as it is sensitive to extreme values. Moreover, in order to avoid biased values, the evaluation of roughness was hereafter limited to those heights values in range of $\pm 0.5 \mu\text{m}$. A comparison between roughness and glossiness can be seen in Fig. 15.

As seen in Fig. 15 no relationship between surface roughness and glossiness could be observed for the range of glossiness selected. Actually this fact was already concluded elsewhere [1]. Some empirical correlations between roughness and glossiness were successfully established for two different types of granites [15]. However, the range of glossiness considered was from 10 up to 90%, and a similar result would be obtained for the granites in case only the range of glossiness from 60 up to 90 % was taken into account.

In order to investigate the roughness at the selected pixels further, new measures of roughness were made by using white light interferometry (WLI). An equipment model NT33 mark Wyko was used. The surface topography was obtained in nanoscale for the centre of each pixel

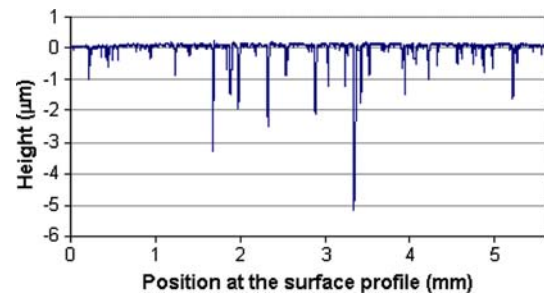
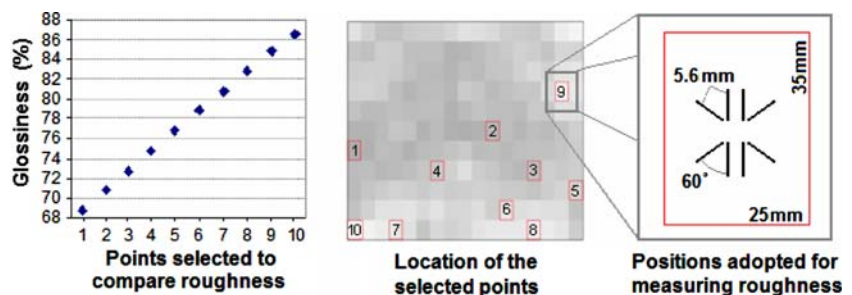


Fig. 14 Typical roughness profile measured

Fig. 13 Experimental approach aiming to compare glossiness and roughness



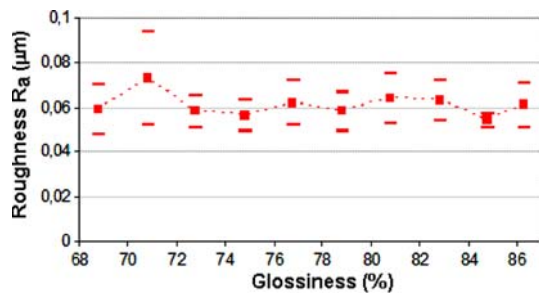


Fig. 15 Comparison of roughness R_a and glossiness

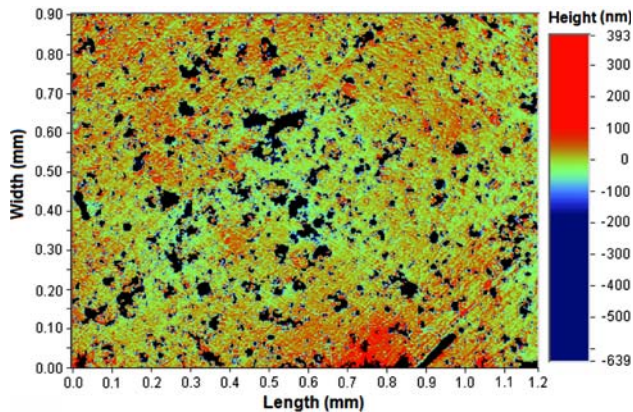


Fig. 16 Surface topography obtained by white light interferometry

considering an area of 0.9×1.2 mm. Result corresponding to 84% of glossiness is presented in Fig. 16.

Topography exposed in Fig. 16 confirms the great smoothness of the polished surface. Surface scratches can still be seen in two different directions, as well as the significant presence of pores with very irregular shape. The values of R_a found were considerably smaller than those measured by profilometry, varying from 30 up to 40 nm as can be seen in Fig. 17.

In spite of the higher accuracy no empirical correlation between glossiness and roughness could be found yet. However, it is very reasonable to expect some influence of pores over the final glossiness. The surface porosity of these regions was then measured, so that a comparison between both surface properties could be established, as shown in Fig. 18.

Unlike for roughness, the differences of surface porosity found could partially explain the variation of glossiness attained for each region in the tile surface. The measurement of porosity was carried out by image analysis. All images were converted into black and white using the software *Adobe Photoshop® CS2*, version 9.0, and the same value of 17 (from 0 up to 255) was adopted as threshold for the identification of pores.

Returning to Fig. 10, the last hypothesis to explain the periodicity of glossiness pattern considers an overlapping

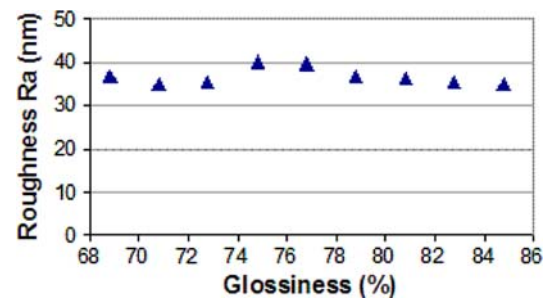


Fig. 17 Comparison of glossiness and the roughness obtained by white light interferometry

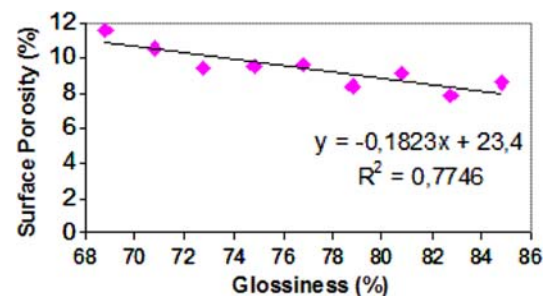


Fig. 18 Correlation between surface porosity and glossiness

of trajectories of subsequent polishing heads, just as detailed previously in Fig. 5. Trajectories of three adjacent polishing heads are presented in Fig. 19, considering the same kinematic conditions used in the polishing process. The distance L between centres of two adjacent polishing heads was taken as 58 cm. At a first look, the significant delay found between these trajectories discards the possibility of a fully constructive interference to be responsible for the wave pattern registered.

Nevertheless, considering the intersection of all zones with less abrasive contact, in the middle of polishing heads, the resulting pattern is hatched in Fig. 20.

A comparison between the pattern of intersection revealed in Fig. 20 and the glossiness pattern furnished by the sequence of tiles was then made and the result is presented in Fig. 21. The region between both delimiting curves represents the area that remains with less abrasive contacts even after the action of three successive polishing heads.

Although the fitting presented in Fig. 10 seems to be more convincing, it must be emphasized that both hypotheses are corroborative. Thus, the glossiness pattern found over the surface of the polished tiles can be reasonably explained by an overlapping of zones with lower abrasive contacts, in addition to a rapid gloss gaining promoted by polishing head with unrepeated abrasive sizes.

Both hypotheses underlie on the premise that the glossiness of a small enough surface portion is somehow

Fig. 19 Difference between trajectories of three adjacent polishing heads during polishing

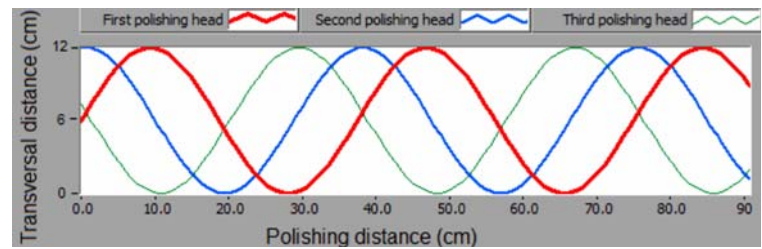


Fig. 20 Intersection of zones with less abrasive contact for three adjacent polishing heads

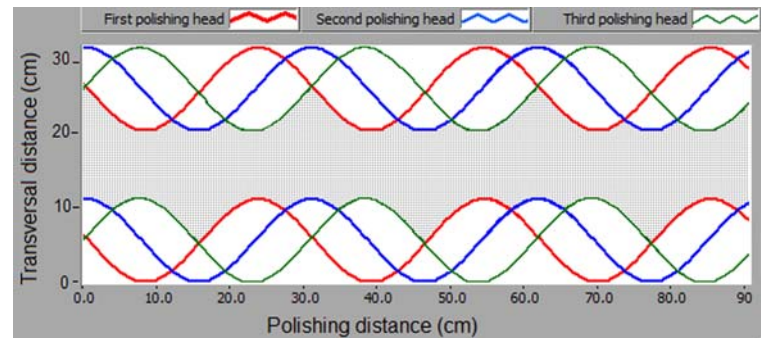
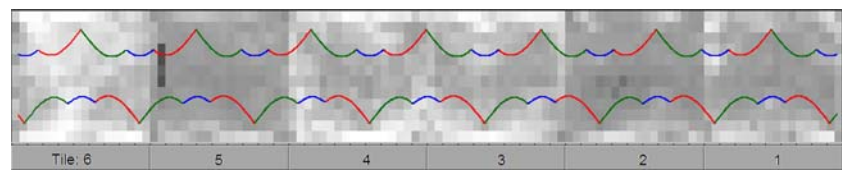


Fig. 21 Lower glossiness left by three adjacent polishing heads



proportional to the number of times abrasives had touched this portion. Actually such premise was already used to explain the glossiness distribution found in stoneware tiles polished with simple polishing machines [4, 5]. However, such proportionality is difficult to assess, since it would depend on several features, either for simple or modern polishing machines. The latter would be especially difficult due to the spatial variation in the number of abrasive contact over the tile surface due to the lateral oscillation motion.

However, lateral oscillation motion can be seen as an extra device that does reduce the biased glossiness pattern typically promoted by simple polishing machines. On the other hand, two other operational parameters are introduced: lateral oscillation frequency and amplitude. These parameters make the polishing kinematics more complicated to optimize, especially by trial and error.

Conclusions

The glossiness pattern due to the polishing process is not homogenous. Significant differences of glossiness were registered either between tiles polished under the same condition, or even within the surface of the same tile. Apart from individual characteristics of the tile this could be

explained by the kinematics adopted during polishing, which causes the number of abrasive contacts to vary.

The use of lateral oscillation motion caused the glossiness to follow a waveform pattern, and two corroborative hypotheses were made in order to explain such fact. The first considers a substantial gloss gaining promoted by one of the final polishing heads, in view of the sensitive behaviour of a light. After the grit 400, the surface roughness of the polished tile approaches $0.2 \mu\text{m}$ and a marked increase of glossiness becomes expected. Therefore this fact must be taken into account during the selection of the abrasive sequence in this range.

The second hypothesis considers an overlapping of trajectories of adjacent polishing heads. The lack of abrasives in the middle of each polishing head was responsible for the small values of glossiness achieved in the central region of the polished tiles.

Correlations between glossiness and roughness could not be established, neither by profilometry nor by white light interferometry. The empirical relationship remains unknown for the porcelain stoneware tiles studied. Nevertheless, a correlation between glossiness and surface porosity was reasonably established for the range of glossiness considered.

Finally, lateral oscillation motion can be seen as an extra device that does reduce the biased glossiness typically

attained when no lateral motion is available. On the other hand, two other operational parameters are introduced: lateral oscillation frequency and amplitude. These parameters make the polishing kinematics more complicated to optimize, especially by trial and error. More studies on the gloss enhancement are needed so that an optimum polishing process could be planned.

Acknowledgements This work was carried out with the support of The National Council for Scientific and Technological Development—CNPq, an entity from the Brazilian Government. Authors would also like to formally thank the Company *Cerâmica Portobello* for supplying the facilities required to carry out this work, as well as Professor Wolfgang Bock, from the Institut für Oberflächen und Schichtanalytik, in Germany, for the measurement with white light interferometer.

References

1. Wang CY, Kuang TC, Qin Z, Wei X (2003) *Am Soc Ceram Bull* 9201–9208
2. Ibáñez MJ, Sánchez E, García-Ten J, Orts MJ, Cantavella V, Sánchez J, Soler C, Portolés J, Sales J (2002) *Qualicer*. Castellón, Spain, pp 32–49
3. Tucci A, Espósito L (2000) *Qualicer*. Castellón, Spain, pp 127–136
4. Hutchings IM, Adachi K, Xu Y, Sánchez E, Ibáñez MJ (2004) *Qualicer*. Castellón, Spain, pp 19–30
5. Hutchings IM, Adachi K, Xu Y, Sánchez E, Ibáñez MJ, Quereda MF (2005) *J Eur Ceram Soc* 3151–3156
6. Hutchings IM, Xu Y, Sánchez E, Ibáñez MJ, Quereda MF (2005) *J Mater Sci* 40:37–42
7. Espósito L, Tucci A, Naldi D (2005) *J Eur Ceram Soc* 785–793
8. Sousa FJP, Aurich JC, Weingaertner WL, Alarcon OE (2007) *J Eur Ceram Soc* 27:3183–3190
9. Lira C (1997) in Academic thesis (Master in Material Science and Engineering)—Post graduation Program in Material Science and Engineering - PGMat, Department of Mechanical Engineering, Federal University of Santa Catarina Florianópolis, Brazil
10. Horiba Instruments Limited, Gloss-Checker IG-320. Equipment datasheet (2007)
11. Sánchez E, Garcia-Ten J, Ibáñez MJ, Orts MJ, Cantavella V (2002) *Am Soc Ceram Bull* 50–54
12. Dondi M, Ercolani G, Garini G, Melandri C, Raimondo M, Rocha E, Almendra E, Tenorio Cavalcante PM (2005) *J Eur Ceram Soc* 25:357–365
13. Su YT, Liu SH, Chen YW (2001) *Wear* 249:808–820
14. Sylvain M (2005) *C R Phys* 6:663–674
15. Huang H, Li Y, Shen JY, Zhu HM, Xu XP (2002) *J Mater Process Technol* 129:403–407